The Separation Dependence of Viscous Damping Coefficients

Jeffrey R. Moffitt

Physics Department, The College of Wooster, Wooster, Ohio 44691

May 2, 2002

A detailed analysis of the effects of viscous drag on the motion of a spinning metal sphere levitated by pressurized nitrogen gas was conducted. Theoretical predictions indicate that the viscous torque should be directly proportional to the angular velocity and inversely proportional to the separation between the sphere and the stand, resulting in an exponential decay of the rotation rate. By monitoring the rotation, the exponential decay coefficients were determined, and by measuring the capacitance of the system, the separation distances were probed. The predicted proportionality between the exponential coefficients and the capacitance values for a given separation is $(5.20 \pm 0.39)\times10^5$ $(\text{Fs})^{-1}$. The observed behavior supported the developed theory with a proportionality of $(2.1 \pm 1.5)\times10^5$ $(\text{Fs})^{-1}$.

INTRODUCTION

Many phenomena in the world around us can be explained with, as Richard Feynman terms it, the behavior of "dry" water, or more clearly: fluid mechanics without the complication of viscosity.[1] Along with the rather simple case of water flowing from a hole in a bucket, complicated phenomenon such as the evolution of vortices[1] or supersonic flow[2] can also be explained without citation to viscosity. However, there are several very simple cases where the dynamics of "dry" water will just not do. For example try to imagine explaining terminal velocity without the sheer strain between the air and the falling object. Situations where the interplay between the fluid and an object or boundary layer which is free to move most often require the addition of viscosity, or "wet" water,[1] into the theoretical considerations, and it is often these situations that are of most interest.

For example, the notion of a "wet" fluid was necessary in the investigation conducted here: the rotational decay of a levitating sphere. This paper will briefly develop an equation of motion for the sphere based on first principles of fluid mechanics. The experimental methods for the testing of theoretical developments will also be discussed along with uncertainty considerations. Finally, a discussion of the observed behavior and some conclusions about the applicability of the developed theory will be made.

THEORY

Newton first postulated that if a velocity gradient is established in a fluid, say along the *x* direction, then the sheer stress in the *y* direction due to the velocity in the *x* direction, S_{xy}, will be proportional to the gradient of the velocity, u_x, at that point.[2] The proportionality constant, η, is the viscosity of the fluid.

$$S_{xy} = \eta \frac{\partial u_x}{\partial y} \qquad (1)$$

For initial simplicity, let us consider the case of two parallel plates separated by a distance, *L*, with the top plate moving at a velocity, *v*. Though it is not necessarily self-evident, the velocity of the fluid immediately beside both of the plates will be exactly that of the nearby plate.[2] By combining these boundary conditions with Eq. (1) and recalling that the sheer stress is equal in magnitude but opposite in direction to the force per unit area required to keep the top plate moving, an equation for the viscous force is derived.[2]

$$F_v = -\eta \frac{v}{L} A \qquad (2)$$

While this relation was derived using two parallel plates, almost all surfaces can be considered to be locally flat in the limit, so Eq. (2) can be utilized in the analysis of many varied geometries.

For example, one case is a spherically symmetric ball rotating on a pocket of gas resting in a spherical base. While the two surfaces of the sphere and the base are not parallel plates, in the limit of infinitesimal areas the curvature of the

plates vanishes, and the viscous forces on each differential area can be modeled with Eq. (2). Because of the geometry the viscous torque at each *dA* is:

$$d\tau = -\eta \frac{v}{L} r dA \qquad (3)$$

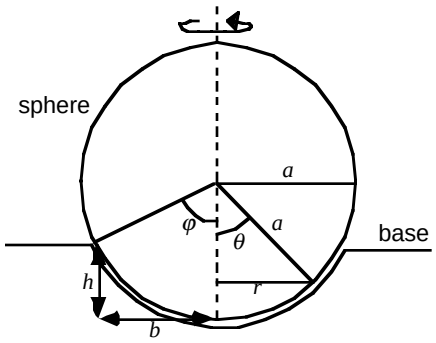

Figure 1: The parameterization used to simplify the problem of determining the viscous torque on a rotating sphere.

Dealing with infinitesimal areas is not a convenient parameterization of the problem, however, so the parameterization seen in Figure 1 is introduced. Here θ is the variable with which *r* will be defined, *a* is the radius of the sphere, φ is the angle where *r* is equal to the radius of the opening of the base, *b*, and *h* is its depth. In this parameterization Eq. (3) becomes:

$$d\tau = -2\pi a^4 \frac{\eta\omega}{L} \sin^3\theta d\theta \qquad (4)$$

Eq. (4) must be integrated to determine the total viscous torque on the rotating sphere. The integration is done from an angle of 0 radians to φ to account for the limited surface over which the viscous torque will act. Defining the integral of the sine-cubed term as the numerical factor, *B*, the viscous torque becomes:

$$\tau = -2\pi a^4 B \frac{\eta\omega}{L} \qquad (5)$$

In a rotating system that is not driven, the torque described in Eq. (5) will cause the rotation rate of the sphere to decay. Newton's second law in angular form, $I\dot{\omega} = \tau$, yields the equation of motion for the system. Inserting the moment of inertia of a rotating sphere of mass, *m*, and radius, *a*, $I = 2/5\, ma^2$, and then using separation of variables, yields the following function of time:

$$\omega = \omega_0 e^{-kt} \qquad (6)$$

where:

$$k = 5\pi B \frac{a^2\eta}{mL} \qquad (7)$$

It should be noted that changing the units of ω will not affect the coefficient of the exponent, *k*, so the rotation may be measured in any fashion without affecting the dependence of Eq. (6) on *L*.

While Eq. (6) dictates the behavior that will be observed for the rotation as a function of time, the work done here also dealt with the *L* dependence of *k*. Because *L* was difficult to observe directly, capacitance measurements were used to determine it. The capacitance between two parallel plates[3] is:

$$C = \frac{\varepsilon_0 A}{L} \qquad (8)$$

To first approximations, the sphere and base can be treated as parallel plates, neglecting boundary affects. The surface area of the plates, *A*, is simply the surface of the sphere which rests in the base. The equation for the surface area of a portion of a sphere is $A = 2\pi a h$, where *h* can be determined to be $h = a - \sqrt{a^2 - b^2}$ (see Figure 1).

Eq. (8) is a valid indicator of *L* only if there is no capacitance inherent in the non-levitating system. In other words, if *L* approaches zero and the system demonstrates a finite capacitance, then the capacitance values measured for the system will reflect the influence of an inherent capacitance, C_0. This can be accounted for by considering the system as two capacitors in series[3]: the first having an *L* dependence as indicated by Eq. (8) and the second as a constant capacitor of capacitance, C_0. The separation dependant capacitance, *C*, will be related to the effective capacitance, C_{eff}, measured for the system by:

$$C = \frac{C_{eff} C_0}{C_0 - C_{eff}} \qquad (9)$$

It is *C* that will be related to the exponential decay coefficient of the sphere.

Since Eq. (7) and Eq. (8) indicate that both *k* and *C* are inversely proportional to *L*, the relationship between *k* and *C* must be directly proportionality, i.e. $k = RC$. Combining them reveals that the proportionality constant, *R*, between the two is:

$$R = 5\pi B \frac{\eta a^2}{\varepsilon_0 A m} \qquad (10)$$

It is the observed rotational decay and the observed value for *R* that can be used to test the theory developed here.

EXPERIMENTAL

A steel sphere with a steel rod perpendicular to its surface was levitated in an aluminum stand designed to fit the curvature of the sphere well. Nitrogen gas was used to levitate the ball, which was then spun and aligned by hand so that the rod was perpendicular to the table surface. A Matheson Regulator, model number IL-580, was used to control the pressure supplied to the stand. The flow valve of the regulator was opened completely for each run.

The rotation rate of the steel sphere was measured by monitoring the signal of a reflected laser. Four strips of electrical tape were equally spaced around the sphere. A Uniphase Model 155SL 3mW laser, was suspended from a stand such that its beam intersected the ball within the length of the electrical tape. A focusing lens was used to focus the reflected beam onto a phototransistor. As the electrical tape rotated through the incident laser beam, the intensity of the reflected beam would drop, causing the voltage across the phototransistor to increase. A Schmitt trigger then produced a TTL compatible signal that was readable by a HP 5385A frequency counter. The frequency counter was controlled by a LabView 4.1 program, which took control of the HP Frequency counter, turned on the filter option, and averaged the rotation rate over 10 s. It then corrected for the 4 strips of electrical tape by dividing the data from the frequency counter by 4.

The capacitance of the system was measured with a GenRad 1657 RLC Digibridge set to treat the resistance as in series and to a frequency of 1 kHz. A stand was used to prevent the weight of the alligator clips and the wiring from affecting the separation distance.

The pressure values on the Matheson regulator gauge were calibrated by a Viatron pressure transducer. The pressure was determined by the voltage from the transducer. An atm of pressure corresponded to each 4.7 mV measured. Once the voltage values were collected, a standardization curve was created between the gauge pressure and atmospheric pressure allowing conversion from one to the other.

All rotation and capacitance data were analyzed using IgorPro. The data were modeled assuming the motion to be described by Eq. (6). The exponential curve fitting function provided by IgorPro was utilized to determine k. The measured capacitance values, C_{eff}, were used to calculate C using Eq. (9). To aid in the estimation of the uncertainty in the calculated values for k, multiple runs were conducted at low pressures, assumed to be the most prone to error, and k values were calculated for all runs using the entire time series and the first half of the time series. These multiple values were used to find average values. The standard deviations were used as an estimation of the uncertainty in the values. Finally, the average k values were plotted against the corresponding C values. A weighted linear curve fit produced the proportionality constant and an estimation of its uncertainty.

RESULTS

The rotational decay of the ball for about 2000 seconds was measured with gauge pressures ranging from 4 psi, the first non-zero mark on the regulator, to 10 psi. A second run was completed for each of the low pressures to aid in determining the uncertainty in these measures. Figure 2 is the rotation data versus time for the run conducted at 10 psi plotted as a semi-log plot. The behavior seen here is representative of the behavior that was exhibited for all pressures.

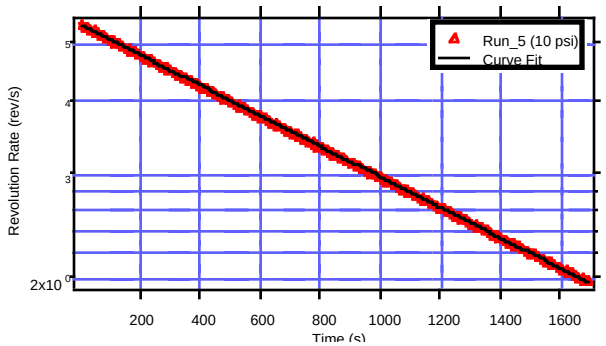

Figure 2: A semi-log plot of rotation data collected at a gauge pressure of 10 psi. The solid line is an exponential fit.

The slope of the apparent linear function, when plotted as a semi-log plot, was the negative of the exponential coefficient k. The values of k for the different gauge pressures are listed in Table I. For all runs k was also determined by fitting an exponential to only the first half points. The average k value for each gauge pressure with the calculated standard deviation as the error bars is plotted against gauge pressure in Figure 3. These values are also listed in Table I. Using Eq. (9) along with the C_0 value measured for the system, 107 ± 1 pF, the L dependent capacitances, C, seen in Figure 4, were calculated. The increase in the error bars is due to an increasing sensitivity of the low pressure C values to the uncertainty in C_0.

Table I: Exponential coefficient values determined through curve fitting of the complete time series and the first half of each time series. These values are listed with the value of the pressure of each run. Also listed are the average of these values and their standard deviation. N/A indicates that a second run was not performed. Actual pressures are known to ± 0.002 atm.

Pressure Value		Complete Data		First Half of Data		Statistical Analysis	
Gauge Pressure	Actual Pressure	First Run k x10^4 s^{-1}	Second Run k x10^4 s^{-1}	First Run k x10^4 s^{-1}	Second Run k x10^4 s^{-1}	Average k x10^4 s^{-1}	STD x10^4 s^{-1}
4 psi	1.16 atm	7.90	8.47	8.21	8.74	8.33	0.36
5 psi	1.24 atm	6.29	6.52	6.44	6.67	6.48	0.16
6 psi	1.31 atm	6.18	6.14	6.31	6.25	6.22	0.07
7 psi	1.38 atm	6.08	N/A	6.20	N/A	6.14	0.08
8 psi	1.46 atm	5.97	N/A	6.14	N/A	6.06	0.12
9 psi	1.53 atm	6.06	N/A	6.26	N/A	6.16	0.14
10 psi	1.60 atm	5.97	N/A	6.01	N/A	5.99	0.03

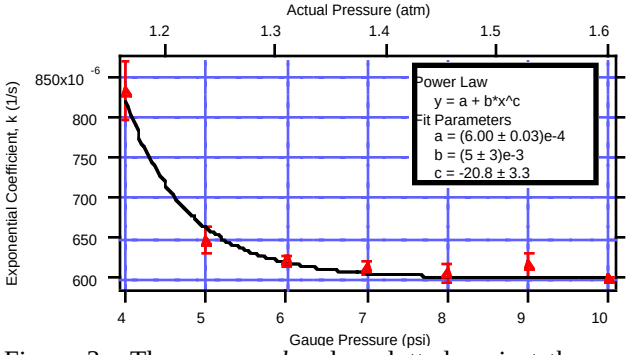

Figure 3: The average k value plotted against the gauge pressure at which each was determined and the actual pressure that the regulator produced at each gauge pressure. The power law used to fit the k values to the actual pressure values is listed along with the parameter values and their uncertainties.

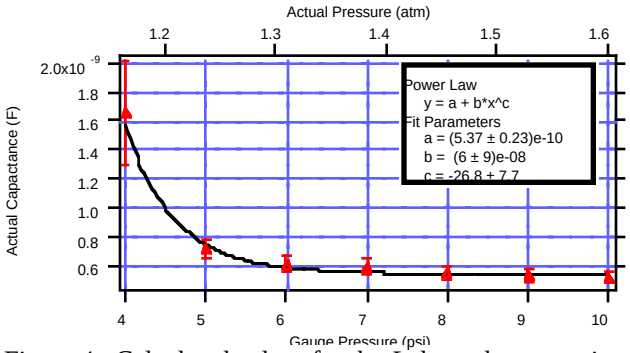

Figure 4: Calculated values for the L dependant capacitance versus the gauge pressure and the corresponding actual pressure. The power law fit and its parameters are listed in the plot.

Table II includes all of the physical measurements of the sphere and stand, the calculated value for φ and h, and the accepted value for the viscosity of nitrogen gas at 300 K and 0.1 Mbar. Using Eq. (10) the predicted value of R was calculated to be $(5.20 \pm 0.39)\text{x}10^5$ $(\text{Fs})^{-1}$. Figure 5 presents the relationship between the values experimentally observed for C and k. The error bars are the standard deviation observed in the k values and the uncertainty in the C values propagated into k. The observed value of R is taken from the slope of the linear fit. It is $(2.1 \pm 1.5)\text{x}10^5$ $(\text{Fs})^{-1}$.

Table II: Measured, calculated, and accepted values needed for analysis.

Variable	Value
Radius of sphere, a (m)	0.05072 ± 0.00008
Radius of stand, b (m)	0.0442 ± 0.0001
Mass of sphere, m (kg)	4.140 ± 0.002
φ (rad) ArcSin[b/a]	1.058 ± 0.007
Depth of stand, h (m)	0.0258 ± 0.0002
Numerical Factor, B	0.215 ± 0.004
Surface Contact Area, A, (m^2)	0.00822 ± 0.00008
Viscosity[4] of N_2, η @ 300K and 0.1 Mbar (Ns/m^2)	(18.0 ± 1.3) x 10^{-6}

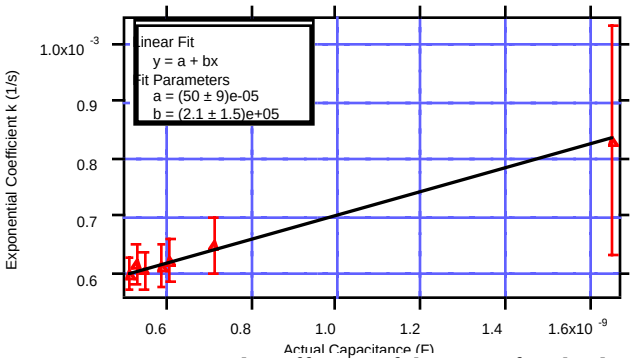

Figure 5: Exponential coefficient of the curve fits, k, plotted against the corresponding capacitance, C. The error bars reflect the uncertainty in k and in C and were used to weight the linear fit. The parameters of the fit are listed in the plot.

ESTIMATION OF UNCERTAINTY

The uncertainty in the predicted value of R for the system arises in part from the uncertainties in the values of the radius of the rotating sphere, a, and in the radius of the base, b. Both of these values were measured three times using a set of calipers. The average value is the reported value, and the uncertainty is the standard deviation in these values. The uncertainties in a and b were then propagated to φ, B, h, and A.

R is also sensitive to the uncertainty in η due to the unknown pressure and temperature of the nitrogen. While η does not vary significantly with pressure, the variations due to temperature are significant.[4] The estimated uncertainty in η corresponded to roughly 25 K of temperature uncertainty, a conservative estimate. This value is listed in Table II. Finally, all of these uncertainties were propagated into the predicted value of R.

Since the uncertainty of the observed value for R was taken from the weighted linear fit of the observed k values versus the observed C values, it was necessary to determine the uncertainty in k and C. To aid in the estimation of the certainty of the k values several things were done. The first was to replicate the runs at low gauge pressures. The second was to calculate the k values from the first half of the data, thus making the k values more sensitive to overall fluctuations in the system. The standard deviation of all of these values was used as a quantitative estimation of this uncertainty.

The uncertainties in the measured capacitance were determined directly from the noise seen by the RLC digibridge. The noise was generally ± 0.001 nF and did not appear to change in magnitude over the range investigated. This was also the uncertainty seen in the value of C_0. These uncertainties were then propagated into C. Finally, the estimated uncertainties in C were propagated into k so that the linear fit of k and C could be properly weighted.

DISCUSSION AND CONCLUSIONS

The first support for the theory developed here is that the rotational damping observed is fit very well by an exponential function. This is indicated by the excellent agreement between the curve fit and the data in Figure 2, and it supports the qualitative conclusion that the rotational viscous torque varies as ω to the first power. Thus, the damping is analogous to Stoke's damping.

The inverse proportionality between k and L was also supported by the observed relationship between k and C. Figure 5 indicates that the k values are well fit by a straight line when plotted against the corresponding C values for a specific pressure. This is strong support for the predicted linear behavior. It should be noted, however, that the significant increase in the error bars at higher values of C might also allow the data to be well fit by other functions. So while there is strong qualitative evidence that the linear relationship between k and C is correct, this evidence is not entirely conclusive.

The greatest support for the theory developed here is the quantitative agreement between the observed R value, $(2.1 \pm 1.5)\text{x}10^5$ $(\text{Fs})^{-1}$, and the predicted R value, $(5.20 \pm 0.39)\text{x}10^5$ $(\text{Fs})^{-1}$. Since the uncertainty in the observed value of R can account for the observed discrepancy between these values within two standard deviations, then it can be concluded that the observed behavior supports the predicted behavior.

[1]R. Feynman, R. Leighton, M. Sands, The Feynman Lectures in Physics, (Addison-Wesley Publishing Co., Reading, 1964)

[2]T. Faber, Fluid Dynamics for Physicists, (Cambridge University Press, Cambridge, 1995)

[3]D. Halliday, R. Resnick, J. Walker, Fundamentals of Physics, 5th Ed. (John Wiley & Sons, Inc., New York, 1997)

[4]D. Lide ed., The Handbook of Chemistry and Physics, 77nd Ed., (CRC Press, Boca Rotan, 1996)